

Zebrafish *colourless* encodes *sox10* and specifies non-ectomesenchymal neural crest fates

Kirsten A. Dutton^{1,*}, Angela Pauliny^{1,*}, Susana S. Lopes¹, Stone Elworthy¹, Tom J. Carney¹, Jörg Rauch², Robert Geisler², Pascal Haffter² and Robert N. Kelsh^{1,‡}

¹Department of Biology and Biochemistry, University of Bath, Claverton Down, Bath BA2 7AY, UK

²Max-Planck-Institut für Entwicklungsbiologie, Spemannstraße 35/III, D-72076 Tübingen, Germany

*These authors contributed equally to this work and are to be considered joint first authors

‡Author for correspondence (e-mail: bssrnk@bath.ac.uk)

Accepted 24 July 2001

SUMMARY

Waardenburg-Shah syndrome combines the reduced enteric nervous system characteristic of Hirschsprung's disease with reduced pigment cell number, although the cell biological basis of the disease is unclear. We have analysed a zebrafish Waardenburg-Shah syndrome model. We show that the *colourless* gene encodes a *sox10* homologue, identify *sox10* lesions in mutant alleles and rescue the mutant phenotype by ectopic *sox10* expression. Using iontophoretic labelling of neural crest cells, we demonstrate that *colourless* mutant neural crest cells form ectomesenchymal fates. By contrast, neural crest cells which in wild types form non-ectomesenchymal fates generally fail to migrate and do not overtly differentiate.

These cells die by apoptosis between 35 and 45 hours post fertilisation. We provide evidence that melanophore defects in *colourless* mutants can be largely explained by disruption of *nacre/mitf* expression. We propose that all defects of affected crest derivatives are consistent with a primary role for *colourless/sox10* in specification of non-ectomesenchymal crest derivatives. This suggests a novel mechanism for the aetiology of Waardenburg-Shah syndrome in which affected neural crest derivatives fail to be generated from the neural crest.

Key words: *Danio rerio*, Waardenburg-Shah syndrome, Hirschsprung's disease, Pigment cells, Melanophore, Apoptosis

INTRODUCTION

The neural crest is a vertebrate tissue of developmental and medical importance. Developmentally, neural crest is intriguing because the cells are initially multipotent and subsequently form a great diversity of derivative cell types, including ectomesenchymal fates, such as craniofacial skeleton and fin mesenchyme, and non-ectomesenchymal fates, such as neurones, glia and pigment cells (Le Douarin, 1982; Smith et al., 1994). Medically, neural crest is important because some diseases, known as neurocristopathies and including diverse conditions such as albinism, neurofibromatosis and Hirschsprung's disease (aganglionic megacolon), affect cell types derived from this tissue (Bolande, 1974).

Understanding the genetic and embryological basis of neurocristopathies has depended on animal models. Thus, models for Hirschsprung's disease, in which individuals have few or no enteric ganglia in the colon, or the related Waardenburg-Shah syndrome, in which individuals combine Hirschsprung's disease with pigmentary anomalies of the skin, hair and irises, have been described in several species, including mouse and zebrafish (Hosoda et al., 1994; Kelsh and Eisen, 2000). Analysis of such models in mice has identified three loci that are crucial for Waardenburg-Shah syndrome

(Attié et al., 1995; Edery et al., 1996; Hofstra et al., 1996; Pingault et al., 1998; Puffenberger et al., 1994; Southard-Smith et al., 1999). Thus, mutations in loci encoding the G-protein-coupled transmembrane receptor protein endothelin receptor B (*Ednrb*) or its natural ligand endothelin 3 (*Edn3*) result in aganglionosis of terminal gut in homozygous mutants (Baynash et al., 1994; Hosoda et al., 1994), as do heterozygous mutations in the *Sry*-related transcription factor gene *Sox10* (Herbarth et al., 1998; Southard-Smith et al., 1998). Homozygous *Sox10* mutant animals show a more severe phenotype with aganglionosis of the whole gut (Herbarth et al., 1998; Southard-Smith et al., 1998). Additionally, mutations in all these genes affect body pigmentation (Lane and Liu, 1984; Mayer, 1965; Mayer and Maltby, 1964), but only *Sox10* mutations result in widespread peripheral nervous system defects (Herbarth et al., 1998; Kapur, 1999; Southard-Smith et al., 1998).

The Sox gene family encodes a large family of transcription factors, with vertebrates likely to have more than 20 Sox genes each (Wegner, 1999). Their precise roles are not well understood, although many are presumed to function in cell fate specification (Pevny and Lovell-Badge, 1997). For example, the founding family member, *Sry*, is likely to be responsible for Sertoli cell specification, and thus male sex

determination, in mammals. While *Sox10* is clearly an important transcriptional regulator in neural crest cell (NCC) development, the cellular basis of the *Sox10* mutant phenotype remains unclear. It has been suggested that peripheral nervous system and pigmentation defects result from loss of NCCs (Southard-Smith et al., 1998; Kapur 1999), although the developmental status of these cells at the time of loss is unknown. Furthermore, roles in defining regional identity in the cranial neural crest and in glial cell differentiation have also been proposed (Bondurand et al., 1998; Herbarth et al., 1998; Kuhlbrodt et al., 1998a; Pusch et al., 1998; Southard-Smith et al., 1998; Britsch et al., 2001).

Mutations at the *colourless (cls)* locus have been identified in zebrafish mutagenesis screens (Kelsh et al., 1996; Malicki et al., 1996). We have previously characterised the crest derivative defect displayed by *cls* mutants (Kelsh et al., 2000a; Kelsh and Eisen, 2000), noting extensive loss of pigment cells and enteric nervous system, together with large reductions in sensory and sympathetic neurones and putative satellite glia and Schwann cells. By contrast, we found little effect on ectomesenchymal derivatives, craniofacial skeleton and fin mesenchyme. Based on the severity and details of the phenotype, we proposed that *cls* functions in specification, proliferation or survival of a progenitor(s) for all non-ectomesenchymal crest derivatives.

The *cls* phenotype, and the cell-autonomy of *cls* gene action in pigment cell types (Kelsh and Eisen, 2000), suggested *sox10* as a candidate gene. We provide an experimental test of this hypothesis. We report the mapping of the *cls* locus and cloning of a zebrafish *sox10* homologue. We show linkage between *cls* and *sox10*, identify *sox10* lesions in four mutant alleles and show rescue of the *cls* phenotype by *sox10* expression. In addition, we describe iontophoretic labelling experiments to examine the precise cell-biological role of *cls/sox10* gene function in neural crest development. We show in live embryos that NCC clones in *cls* and wild-type embryos differentiated into ectomesenchymal fates after migration to appropriate sites. Remaining NCC clones adopted non-ectomesenchymal fates in wild-type embryos. By contrast, in *cls* embryos differentiation to non-ectomesenchymal fates was rarely observed. Instead, most clones failed to migrate and underwent late cell death by an apoptotic mechanism. Finally, for the melanophore fate, we show disrupted expression in *cls* mutants of genes vital for melanophore specification and migration. Together, these data demonstrate a complex phenotype in *cls* embryos that can be explained by proposing that *cls/sox10* has a primary role in specification of non-ectomesenchymal fates. Defects in cell migration, survival and differentiation are therefore likely to be secondary consequences of an inability of these cells to adopt specific fates.

MATERIALS AND METHODS

Fish husbandry

Embryos were obtained through natural crosses and staged according to Kimmel et al. (Kimmel et al., 1995). We used 4 *cls* alleles (*m618*, *t3*, *tw2* and *tw11*).

Mapping of *cls*

cls^{tw11} heterozygous fish (Tübingen background), were crossed to wild-type strain WIK11 to produce a reference mapping cross.

Heterozygous F₁ were incrossed and separate pools of F₂ homozygous *cls* fish and their wild-type siblings were used for simple sequence length polymorphism analysis (Knapik et al., 1996). Linkages from the pools were confirmed and refined by genotyping individual embryos, as described by Rauch et al. (Rauch et al., 1997).

Isolation, sequencing, phylogenetic analysis and radiation hybrid mapping of zebrafish *sox10*

RT-PCR was performed using total RNA of 19 hpf stage wild-type embryos using published conditions and degenerate primers (Yuan et al., 1995). Sequencing of resulting clones identified a *sox10*-like sequence. The *sox10* clone was extended by RACE PCR using gene-specific primers (Clontech, SMART RACE kit) and sequenced on an ABI DNA sequencer. All primer sequences available on request. The full *sox10* cDNA sequence is available in Genbank (Accession Number AF402677). The zebrafish *sox10* homologue was mapped on the radiation hybrid panel LN54 (Hukriede et al., 1999) by PCR with primers 5'-ACCGTGACACACTCTACCAAGATGACC-3' and 5'-CATGATAAAATTTGCACCCTGAAAAGG-3', which generate a 931bp 3' UTR fragment.

For phylogenetic analysis sequences were extracted from Genbank and coding sequences automatically extracted using Genetrans (within GCG9). These were translated and then aligned using ClustalX (Thompson et al., 1997). The nucleotide alignments were reconstructed from the protein alignments using MRTRANS (www.hgmp.mrc.ac.uk/Registered/Option/mrtrans.html). Tree-Puzzle (v 4.0.2) was used to construct an unrooted tree by maximum likelihood (Strimmer and von Haeseler, 1996). It automatically assigns estimations of support to each internal branch, figures for which are presented in the figure. To model the substitution process the Tamura and Nei (Tamura and Nei, 1993) model was employed and all sites were used. Gamma distributed variation in rates of evolution was permitted with eight variable sites and one invariable. Parameters were estimated using quartet sampling and the neighbour-joining tree.

Characterisation of mutant *sox10* alleles

Total RNA from 27 hpf homozygous embryos of mutant alleles *cls^{m618}*, *cls^{tw2}* and *cls^{tw11}* was prepared using TRI reagent (Sigma). First strand cDNA was generated using random hexamers and SuperscriptII RT (GibcoBRL). For each allele four overlapping RT-PCR fragments were sequenced to identify mutant lesions. For *t3*, genomic DNA was extracted from individual *cls^{t3}* mutant embryos, a genomic fragment encoding the N-terminal of the Sox10 protein was amplified by PCR and sequenced commercially (Oswell, Southampton). The *t3* insertion sequence is available in Genbank (Accession Number, AF404490).

Ectopic expression in zebrafish embryos

The full coding region of *cls^{m618}* was amplified by RT-PCR using primers *Clal*-S21 (5'-CCATCGATACCTACCGAAGTCACCTGTGG-3') and S27-*XbaI* (5'-GCTCTAGAGTTTGTGTGCGATTGTGGTGC-3'). The 1615bp fragment was subcloned into the *Clal/XbaI* site of the heatshock vector pCSHSP (Halloran et al., 2000) to generate hs>*sox10(L142Q)*. The wild type *sox10* construct, hs>*sox10*, was generated by site-directed mutagenesis of hs>*sox10(L142Q)* using QuikChange Site Directed Mutagenesis Kit (Stratagene). Sequencing confirmed the successful generation of both clones. DNA purified for injection using Microcon Filter Devices (Millipore) was diluted to a concentration of 25 ng/μl, with 0.1% Phenol Red. *cls^{m618}* or their wild-type siblings were injected with 2 nl of either hs>*sox10* or hs>*sox10(L142Q)* at the one- to two-cell stage and incubated at 28.5°C. As appropriate, embryos were heatshocked twice (at 10-13 hpf and 22-24 hpf), by incubation at 37°C for 1 hour. *cls* embryos were scored for rescue at 48 hpf using a MZ12 dissecting microscope (Leica). Rescue was defined as the presence of at least one melanophore of wild-type morphology; these are never seen in uninjected mutant embryos.

Intophoretic labelling and clonal analysis of single neural crest cells

Intophoretic labelling of individual neural crest cells was performed using essentially the method of Raible et al. (Raible et al., 1992), except that micropipette tips were filled with 3% lysinated rhodamine dextran and 3% biotinylated dextran (both $10 \times 10^3 M_r$; Molecular Probes) mixture dissolved in 0.2 M KCl and the needles backfilled with 0.2 M KCl. Embryos from heterozygotes for *cls* alleles *t3*, *tw2* and *tw11* were used; no phenotypic differences between these alleles were seen, so we do not distinguish them here. Individual NCCs were labelled by intracellular injection with dye. Premigratory cranial crest cells, between the posterior eye and the anterior boundary of somite 1, were labelled in 4-14 somite (11-16 hours post fertilisation, hpf) embryos, while premigratory trunk NCCs at the level of somite 7 were labelled in 16-22 somite (18-20 hpf) embryos. Premigratory trunk NCCs at the level of somite 14 were labelled in 22-25 somite (20-22 hpf) embryos. Embryos were recovered and raised for several hours at 28.5°C in embryo medium with 1% v/v penicillin/streptomycin solution (Gibco). Embryos were remounted and examined to identify those with only a single labelled NCC; only these embryos were analysed.

Labelled cells were monitored using Nomarski and fluorescence optics on a BX50WI microscope (Olympus), and documented on a Eclipse E800 microscope (Nikon) using low light level, video-enhanced fluorescence microscopy. Labelled cells were monitored twice daily for up to 3 days until progeny could be identified using published morphological criteria (Raible and Eisen, 1994; Raible et al., 1992; Schilling and Kimmel, 1994). Thus, melanophores contained melanin granules; xanthophores were visibly yellow and autofluoresced at a wavelength near that of fluorescein; iridophores contained iridescent granules; dorsal root ganglial neurones were identified by position ventrolateral to the neural tube combined with a visible neurite; sympathetic neurones were positioned ventral and lateral to the notochord and showed neurites; Schwann cells were elongated and positioned along axonal processes, e.g. trigeminal nerve; satellite glia were associated with the ganglionic sheath or appeared to be wrapped around neuronal stomata; craniofacial cartilage formed characteristic stacks of vacuolated cells in the jaw or gill arches; fin mesenchyme occupied a position within the dorsal fin fold and showed characteristic asymmetric organisation of projections (Smith et al., 1994). Cells which could not be assigned to any of the described groups, owing to their position in regions of limited optical resolution or lack of distinctive morphologies, were classified as 'unidentified'. In cranial regions, these cells undoubtedly included cells of connective tissue fates (Schilling and Kimmel, 1994).

TUNEL

TUNEL (terminal deoxynucleotidyl transferase (TdT)-mediated deoxyuridinetriphosphate (dUTP) nick end-labelling) of double-strand DNA fragmentation was used to confirm apoptosis in cells with apoptotic morphology. *cls^{t3}* and their wild-type siblings were fixed overnight at 4°C in 4% paraformaldehyde and TUNEL performed using fluorescein dUTP and developed using 4-Nitroblue tetrazolium chloride and 5-Bromo-4-chloro-3-indolyl-phosphate (Boehringer Mannheim; Reyes, 1999).

Morpholino injections

AB wild-type embryos at 25, 30 and 35 hpf were injected with either a high (16.5 ng) or low (9 ng) dose of a morpholino designed to knock-down *sox10*, as described previously (Dutton et al., 2001). Effects on *nac/mitf* expression in melanoblasts at 25 hpf were evaluated by counting *nac/mitf*-expressing cells in one half of the trunk in each of 20 embryos at each dose.

Whole-mount in situ hybridisation and antibody staining

RNA in situ hybridisation was performed as described by Kelsh and Eisen (Kelsh and Eisen, 2000), on *cls^{m618}*, *cls^{tw11}* and *cls^{t3}*, their wild-

type siblings and morphants. Probes for the following genes were used: *nac/mitf* (Lister et al., 1999), *spa/kit* (Parichy et al., 1999); *dopachrome tautomerase (dct)* (Kelsh et al., 2000b); *dlx2* (Akimenko et al., 1994); *forkhead 6 (fkd6)* (Odenthal and Nusslein-Volhard, 1998).

Antibody staining with anti-Hu, mAb 16A11 (Marusich et al., 1994), was performed using peroxidase-antiperoxidase (VECTASTAIN® Elite ABC kit) and DAB substrate.

RESULTS

cls and a zebrafish *sox10* homologue map to the same region of Linkage Group 3

The strong phenotypic similarity between *sox10^{D^{om}}* mice and *cls* mutants suggested a zebrafish *sox10* homologue as a candidate gene for *cls*. We used RT-PCR to clone a partial *sox10*-like HMG box and RACE RT-PCR to clone 5' and 3' regions. Sequencing these clones revealed an open reading frame encoding a *sox10* homologue, which we refer to as *sox10* (Fig. 1A,B).

Genetic mapping of 274 meioses placed *cls* on LG 3 within a 3.9 cM interval between markers z872 and z13387 (Fig. 1C). Two oligonucleotide primers amplified a 931 bp fragment from zebrafish, but not from control mouse genomic DNA. Amplification from the DNAs in the LN54 radiation hybrid mapping panel (Hukriede et al., 1999) with these primers mapped *sox10* to LG 3, 0cR from the marker z8492 (LOD score=17.6; Fig. 1C). The striking linkage of *cls* and *sox10*, together with in situ hybridisation experiments showing *sox10* expression in neural crest (see below), strongly supported our hypothesis that *cls* might encode *sox10*.

sox10 is disrupted in *cls* mutants

We used RT-PCR to amplify the *sox10*-coding region from 27 hpf homozygous mutants of 3 *cls* alleles. Sequencing these PCR products identified sequence differences from wild-type consistent with them causing the mutant phenotype (Fig. 1D,E). Two alleles show an A→T transversion, resulting in a premature Stop codon; the third is a non-conservative substitution (L142Q) of a fully-conserved residue in the HMG domain. A fourth allele, *t3*, showed highly reduced RNA expression using a 3' probe for whole-mount RNA in situ hybridisation. PCR from genomic DNA identified a 1.5 kb insertion in all *t3* mutants that was not present in wild types. Sequencing genomic DNA from *t3* homozygotes identified a 1397 bp insertion with sequence homology to a transposon first identified in a mutant *no tail* allele (data not shown; Schulte-Merker et al., 1994). The insertion interrupts the *sox10*-coding sequence upstream of the HMG domain and adds eight novel amino acids before prematurely truncating the protein (Fig. 1D).

To test further whether *cls* encodes *sox10*, we attempted to rescue the *cls* phenotype with ectopic *sox10* expression under heat shock control. We took advantage of the consistent absence of large, stellate melanophores in every *cls* embryo. Ectopic expression of wild-type *sox10* rescued 1-40 melanophores to a wild-type morphology in 48% of *cls^{m618}* mutants, while ectopic mutant *sox10(L142Q)* failed to do so (Table 1; Fig. 2). Furthermore, while *cls* melanophores always remain dorsal to the neural tube, rescued melanophores frequently migrated, even to very distal positions (Fig. 2).

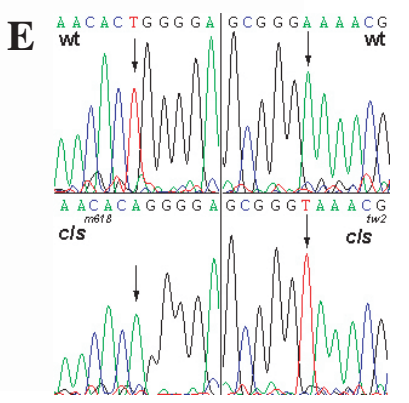
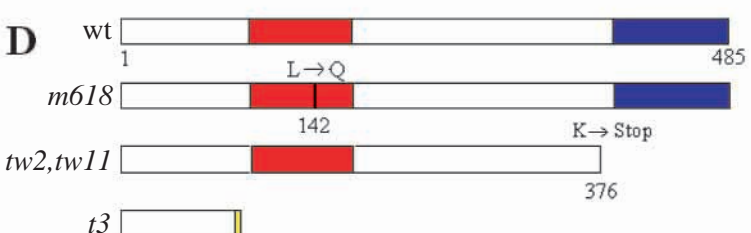
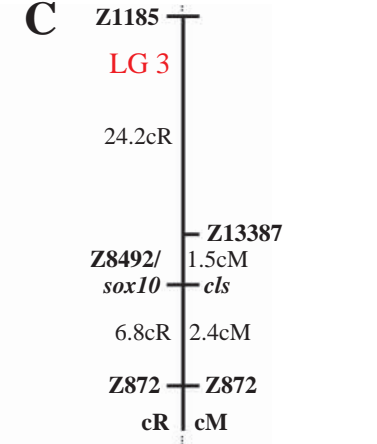
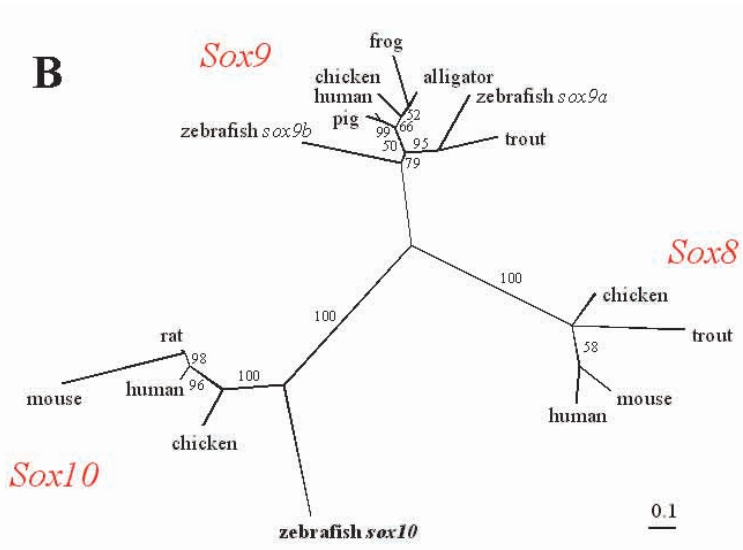
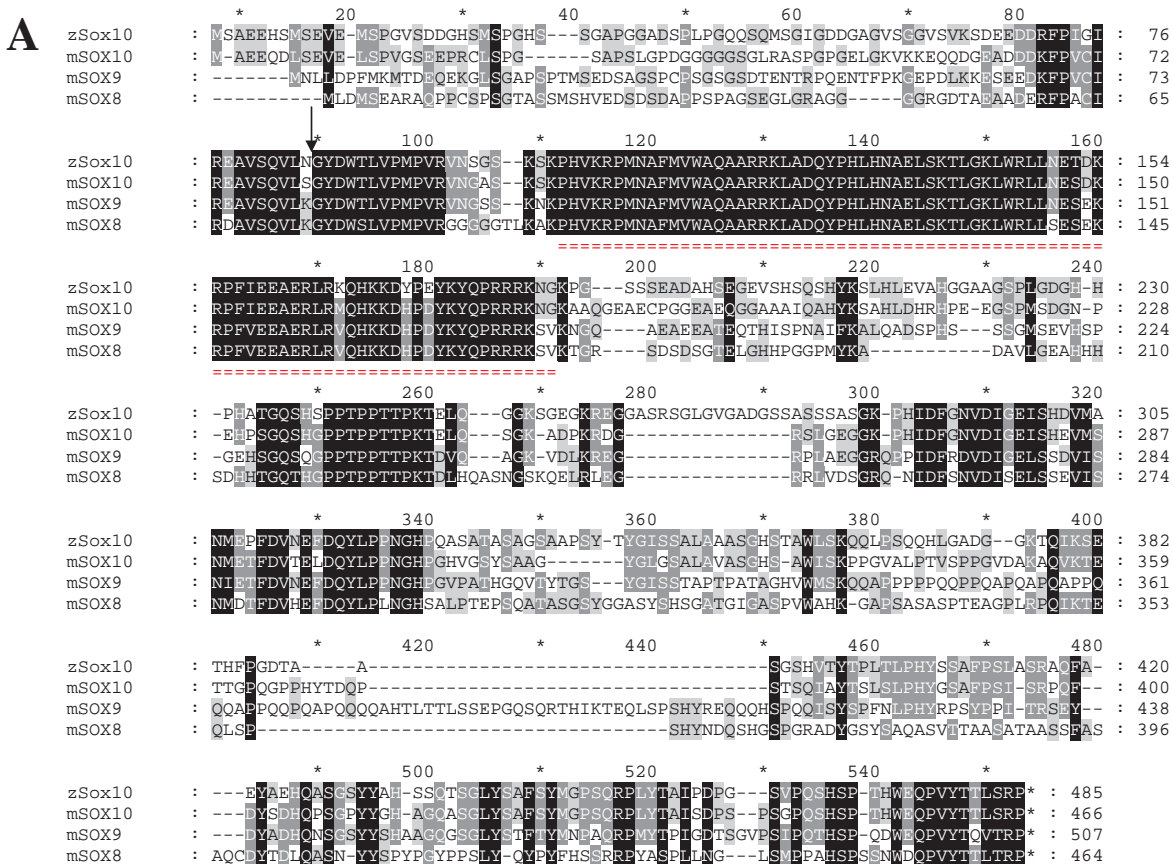


Fig. 1. A zebrafish *sox10* homologue maps to the region of the *cls* locus. (A) Sequence comparison of predicted zebrafish Sox10 homologue (44, 45 and 60% identity to mouse Sox8, Sox9 and Sox10, respectively). Blocks of identity corresponding to all proposed functional domains can be seen, including the HMG domain (red underline; 95% amino acid identity), N-terminal synergy domain (1-105; 48% identity), dimerisation domain (66-105; 78% identity), C-terminal transcriptional activation domain (395-485; 76% identity) and a domain C-terminal to the HMG domain corresponding to a putative protein-protein interaction domain (234-325; 64% identity; Bondurand et al., 2000; Kuhlbrodt et al., 1998a; Kuhlbrodt et al., 1998b; Liu et al., 1999; Peirano and Wegner, 2000). (B) Maximum likelihood phylogenetic tree of subgroup E Sox genes. Zebrafish *sox10* clusters within the *Sox10* clade of vertebrate Sox genes. The Accession Numbers for the sequences are as follows: chicken *Sox8* (AF228664); trout *SoxP1* (D83256); mouse *Sox8* (AF191325); human *SOX8* (AF226675); frog *Sox9a* (AB035887); alligator *Sox9* (AF106572); trout *Sox9* (AB006448); zebrafish *sox9a* (AF277096); zebrafish *sox9b* (AF277097); chicken *Sox9* (AB012236); pig *Sox9* (AF029696); human *SOX9* (Z46629); zebrafish *sox10* (AF402677); chicken *Sox10* (AF152356); mouse *Sox10* (AF047389); rat *Sox10* (AJ001029); human *SOX10* (NM_006941). (C) Mapping using the LN54 panel placed *sox10* on LG 3 in the region of the *cls* locus identified using microsatellite markers (we found four recombinants between *cls* and z13387 in 274 meioses). Note that z8492 was not polymorphic and could not be analysed in the mapping cross. (D) Schematic to illustrate changes in Sox10 mutant proteins. In *cls^{sm618}* a T425A substitution results in a non-conservative change (Leu142Gln) within the HMG domain (red). In *cls^{tw2}* and *cls^{tw11}*, a A1126T substitution introduced a Stop codon truncating the protein just N-terminal to the transactivation domain (blue). Insertion of a 1.4 kb transposon at the site indicated by the arrow in A disrupts *sox10* in *cls^{t3}* and introduces a C-terminal extension of eight novel amino acids before premature truncation N-terminal to the HMG domain (yellow). (E) Chromatogram traces to show nucleotide changes affecting *sox10*-coding regions in *cls^{sm618}* and *cls^{tw2}*.

sox10 expression is disrupted in *cls* mutants

We used *in situ* hybridisation to examine *sox10* expression in wild-type and *cls* embryos. In wild types, expression was first detected at the one-somite stage in cells in the lateral neural plate (data not shown). Throughout somitogenesis stages, strong *sox10* expression was seen in premigratory NCCs and extended progressively more caudally in older stages (Fig. 3A-C,F). Double RNA *in situ* hybridisation studies show that there is extensive, but incomplete, overlap of *sox10* and *fdk6*, a marker expressed widely in premigratory NCCs (Fig. 3O,P) (Odenthal and Nuesslein-Volhard, 1998). *sox10* expression was maintained in some migrating NCCs on the medial migration pathway (Fig. 3C,F). By 30-40 hpf *sox10* expression

Table 1. Rescue of *cls* phenotype using ectopic *sox10* expression

Construct	Heat shock	Injected <i>cls</i> ⁻ that survived	Rescued <i>cls</i> ⁻ (% rescued)	Mean number of melanophores per rescued embryo
<i>hs>sox10</i>	+	92	44 (48)	15
<i>hs>sox10</i>	-	48	17 (35)*	4.3
<i>hs>sox10(L142Q)</i>	+	122	0 (0)	0

*A similar degree of leakiness with this promoter has been reported by Lister et al. (Lister et al., 1999); note that the degree of rescue is much less in the absence of heat shock.

on the medial pathway is organised in segmentally arranged clusters adjacent to the notochord, presumably developing Schwann cells associated with the segmental nerves (Fig. 3Q); *sox10* expression is lost from this site by 48 hpf. Although NCCs are found extensively on the lateral pathway from 24 hpf (Raible et al., 1992), counts of *sox10*-expressing cells show that expression was essentially absent from cells on this pathway (Fig. 3M,N). This demonstrates the rapid downregulation of *sox10* from pigment cell precursors, as NCCs on this pathway form only pigment cells (Raible and Eisen, 1994). Consistent with this, xanthophores and most pigmented melanophores show no detectable *sox10* expression (Fig. 3L), although some weakly expressing melanophores were noted at earlier stages (Fig. 3K). Expression was not seen in fin mesenchyme nor in *dlx2*-expressing craniofacial cartilage precursors (Fig. 3D,E), although differentiating jaw cartilage shows weak expression by 60 hpf (data not shown). Cells expressing *sox10* accumulated in clusters corresponding to the forming cranial ganglia and extending along the posterior lateral line nerve by 24 hpf (Fig. 3F,H), in a pattern reminiscent of *fdk6* expression (Kelsh et al., 2000a), suggesting that *sox10* is expressed in satellite glial and Schwann cells. Consistent with this interpretation, double labelling with anti-Hu antibody confirmed the non-overlapping expression of *sox10* and this neuronal marker (Fig. 3J). *sox10* is maintained in developing Schwann cells on the posterior lateral line nerve up to 60 hpf (data not shown). *sox10* expression was prominent in enteric nervous system precursors at 60 hpf (Fig. 3S).

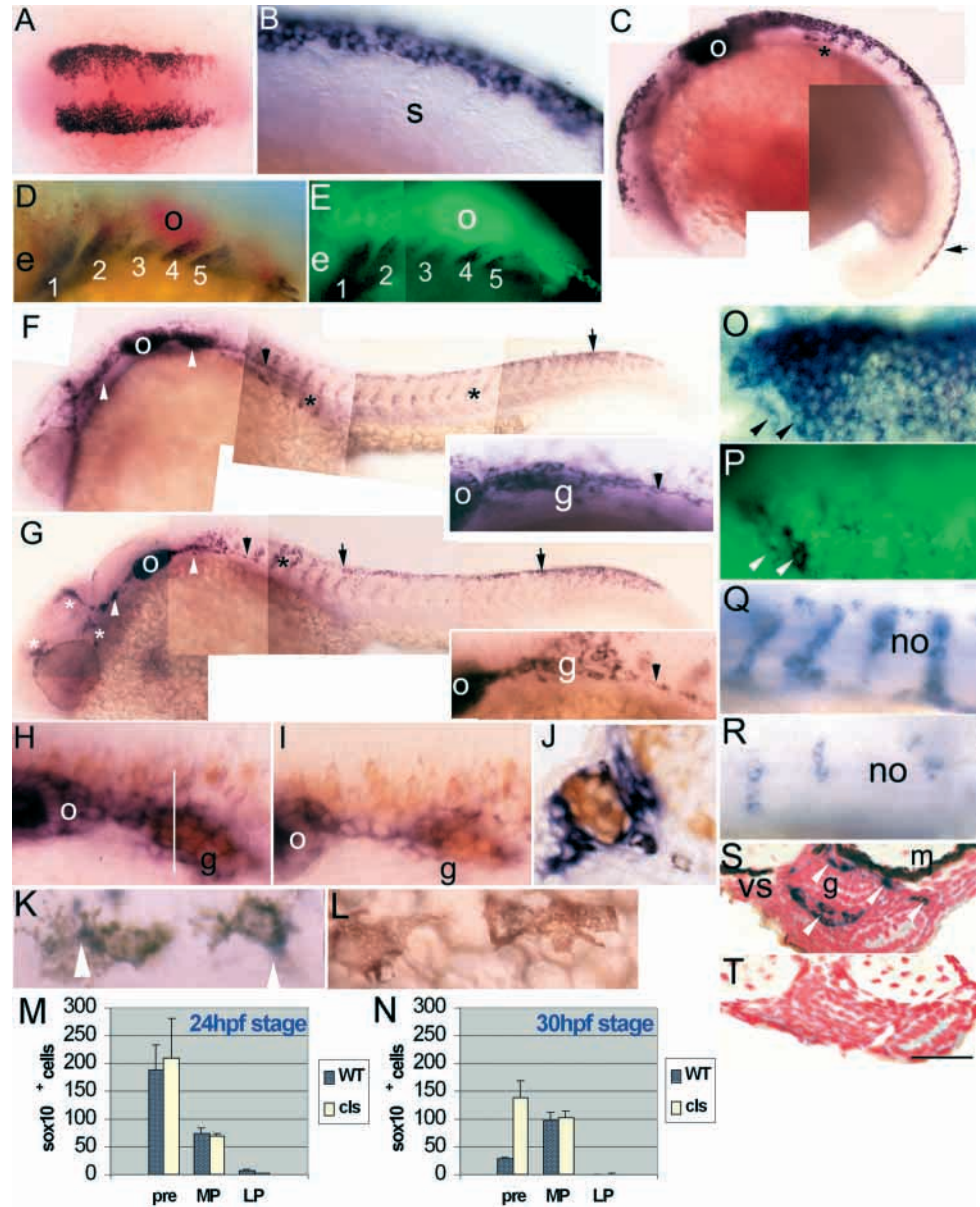
At early stages, premigratory crest showed equivalent patterns of *sox10*-positive cells in wild-type and *cls^{tw11}* and *cls^{sm618}* mutant embryos. Counts at 24, 30 and 35 hpf revealed that although in wild type *sox10*-expressing cells were rapidly lost from the premigratory position, they remained here in *cls^{sm618}* mutants; by contrast, *sox10* expression in migrating trunk NCC was broadly comparable between wild type and *cls^{sm618}* mutants (Fig. 3M,N). Additionally, *cls* mutants were

Fig. 2. *cls* phenotype is rescued by ectopic *sox10* expression. Wild-type embryos show many large, strongly pigmented melanophores at 48 hpf (A; close-up of anal region in D), while *hs>sox10(L142Q)*-injected *cls^{sm618}* mutants (B) show only tiny melanised spots in position of premigratory NCCs (arrowheads). (C,E,F) By contrast, *cls^{sm618}* embryos injected with *hs>sox10* and heat-shocked, show mosaic rescue of melanophores. This embryo showed one rescued melanophore in the dorsal stripe (* in C), two in the ventral stripe (arrows in C; close-up in E) and one on the yolk sac (F). Scale bar: 125 µm in A-C; 70 µm in D-F.



Fig. 3. Embryonic *sox10* expression in wild-type and *cls* embryos.

(A,B) *sox10* is expressed in most cranial (A; five-somite stage) and trunk (B; 14-somite stage) premigratory NCCs; double mRNA in situ hybridisation with *fkf6* (O, purple) and *sox10* (P, green) in a six-somite stage embryo reveals extensive overlap, although some individual NCCs lack *sox10* (arrowheads). (C) 18-somite stage embryo shows strong expression in premigratory (black arrow) and migrating (asterisk) NCCs and otic vesicle (o). (D,E) Double mRNA in situ hybridisation with *dlx2* (D, purple) and *sox10* (E, green) in 29 hpf stage embryos shows absence of *sox10* expression in developing branchial arches (1-5). (F) By 24 hpf in wild types, strong expression is associated with cranial ganglia (white arrowheads) and posterior lateral line nerve (black arrowhead; enlarged in inset), otic vesicle (o), migrating NCCs throughout trunk (asterisks) and in premigratory crest (arrow). (G) At 24 hpf in *cls* mutants, expression in the head is clustered (white asterisks) and cranial ganglia have reduced labelling (white arrowheads). Cells expressing *sox10* extend along the posterior lateral line nerve (arrowhead and inset). Rostral trunk shows some migrating cells (black asterisk), but *sox10*-positive cells are clustered dorsal to the neural tube (arrows) in trunk and tail. (H,I) Combined *sox10* in situ hybridisation (purple) and anti-Hu antibody labelling (orange) shows strong *sox10* expression associated with wild-type (H) posterior lateral line ganglion (g), much reduced in *cls* mutant (I). (J) In transverse section of wild-type ganglion (approximate position indicated by white line in H), *sox10* expression is strong peripherally (non-neuronal cells), but absent centrally (neurons). (K,L) 36 hpf wild-type embryos show weak expression in some melanophores, but not all. Thus, weak expression (arrowhead) is seen in some cells of the dorsal stripe (K), but not in cells on the yolk sac (L). (M,N) Number of *sox10*-expressing NCCs in different locations (pre migratory, pre; migrating on medial pathway, MP; migrating on lateral pathway, LP) of trunk and anterior tail (somites 1-20) at 24 (M) and 30 hpf (N) in WT and *cls* mutants. (Q,R) Segmentally arranged lines of *sox10*-positive cells lying adjacent to the notochord (no), presumably glia, are abundant in wild type (Q) and only weakly affected in *cls* mutants (R) at 40 hpf. (S,T) Transverse section of trunk of 60 hpf wild-type embryo (S) shows enteric nervous system expression (arrowheads) lateral to the gut (g), absent in *cls* mutant (T). e, eye; m, muscle; s, somite; vs, ventral stripe melanophores. All images are lateral views, rostral towards the left, dorsal upwards, except dorsal views of A,K,O,P. Scale bar: 200 μ m in A; 50 μ m in B,H-I,K-L; 120 μ m in C; 75 μ m in D,E; 150 μ m in F,G; 35 μ m in J; 65 μ m in O,P; 55 μ m in Q,R; 45 μ m in S,T.



distinguishable from 24 hpf by the clustered, not scattered, distribution of *sox10*-positive cells in the head (Fig. 3F,G) and a variable reduction in the number of *sox10*-positive cells in cranial ganglia and on cranial nerves (Fig. 3H,I). By 35 hpf, *cls* mutants were readily distinguished from wild types by their reduced number of *sox10*-positive cells, concentrated in a premigratory position dorsal to the neural tube or clustered near the posterior lateral line ganglia; putative Schwann cells were missing from the posterior lateral line nerve. *cls* mutants

showed reduced expression in the putative Schwann cells found as segmental clusters of *sox10*-positive cells (Fig. 3Q,R). Enteric nervous system precursors were absent at 60 hpf (Fig. 3T) in *cls* mutants.

In contrast to the other mutant alleles examined, *cls*^{t3} mutants consistently show highly reduced *sox10* transcripts when examined using the 3' *sox10* probe at all stages. When examined using a probe lying 5' to the insertion site, *sox10* expression levels were comparable with those in other mutant

Table 2. Fates of single neural crest cells injected with lineage tracer

Fate [‡]	Trunk (somite 14)				Cranial*			
	Wild type		<i>colourless</i>		Wild type		<i>colourless</i>	
	Number	Percentage	Number	Percentage	Number	Percentage	Number	Percentage
Ectomesenchymal								
Cartilage	–	–	–	–	6	7	2	6
Fin mesenchyme	5	7	2	8	–	–	–	–
Non-ectomesenchymal								
Pigment								
Melanophore	26	34	–	–	12	14	–	–
Xanthophore	9	12	4 [§]	16	12	14	7 [§]	21
Iridophore	3	4	–	–	2	2	–	–
Mixed pigment	10	13	–	–	–	–	–	–
Neural								
Cranial ganglia	–	–	–	–	9	11	–	–
Dorsal root ganglia	6	8	–	–	–	–	–	–
Sympathetic neuron	3	4	–	–	–	–	–	–
Schwann cell	1	1	–	–	–	–	–	–
Mixed neural [¶]	5	7	–	–	–	–	–	–
Mixed pigment/neural								
Melanophore + Dorsal root ganglia	1	1	–	–	–	–	–	–
Other								
Died	1	1	19 [§]	76	11	13	15 [§]	45
Unidentified	5	7	–	–	33	39	9	27
Total	75	100	25	100	85	100	33	100

*All progeny within a single clone adopted the same fate in every case, as shown previously (Schilling and Kimmel, 1994).

[‡]Only single injected cells that survived and were identified as NCCs in the afternoon on the day of labelling are included. The numbers represent the number of clones whose cells adopted the indicated fates, using the criteria outlined in the Materials and Methods.

[§]All xanthophores identified in *cls* embryos subsequently died; hence in total, 23 (92%) and 22 (66%) cells died in the somite 14 and cranial samples.

[¶]Mixed neural fates include clones with both neuronal and glial derivatives.

alleles, suggesting that insertion of the transposon does not disrupt transcription of 5' sequences (data not shown).

Outside neural crest, *sox10* expression was particularly strong in otic placode and otic vesicle, and from 11-somite stage onwards (Fig. 3C,F,H), was detected in pectoral fin and in some spinal cord cells from 36 hpf. Expression in the ear was significantly weaker in *cls* mutants by 40 hpf (data not shown).

***cls* non-ectomesenchymal neural crest cells die prior to differentiation**

Previous characterisation of *cls* embryos catalogued a strong reduction in non-ectomesenchymal neural crest derivatives (Kelsh and Eisen, 2000). To analyse the cell biological basis for loss of these neural crest derivatives, we used iontophoretic labelling of single NCCs. We labelled premigratory NCCs in *cls* mutants and their wild-type siblings in two regions that generate ectomesenchymal fates, and scored them for the fate(s) adopted by their progeny (Table 2). In wild-type embryos, almost all (148/160; 93%) labelled cells survived throughout the experiment, and all major derivatives, both ectomesenchymal and non-ectomesenchymal, were identified among the clones. Consistent with our previous analyses, labelled cells generated a similar proportion of ectomesenchymal fates in *cls* mutants (4/58; 7%) and wild-type siblings (11/160; 7%). Furthermore, even in *cls* mutants, cells in these clones migrated and differentiated normally. In wild-type embryos, most cells where fates were identifiable (111/122; 91%) differentiated into recognisable non-ectomesenchymal derivatives. By contrast, most identifiable

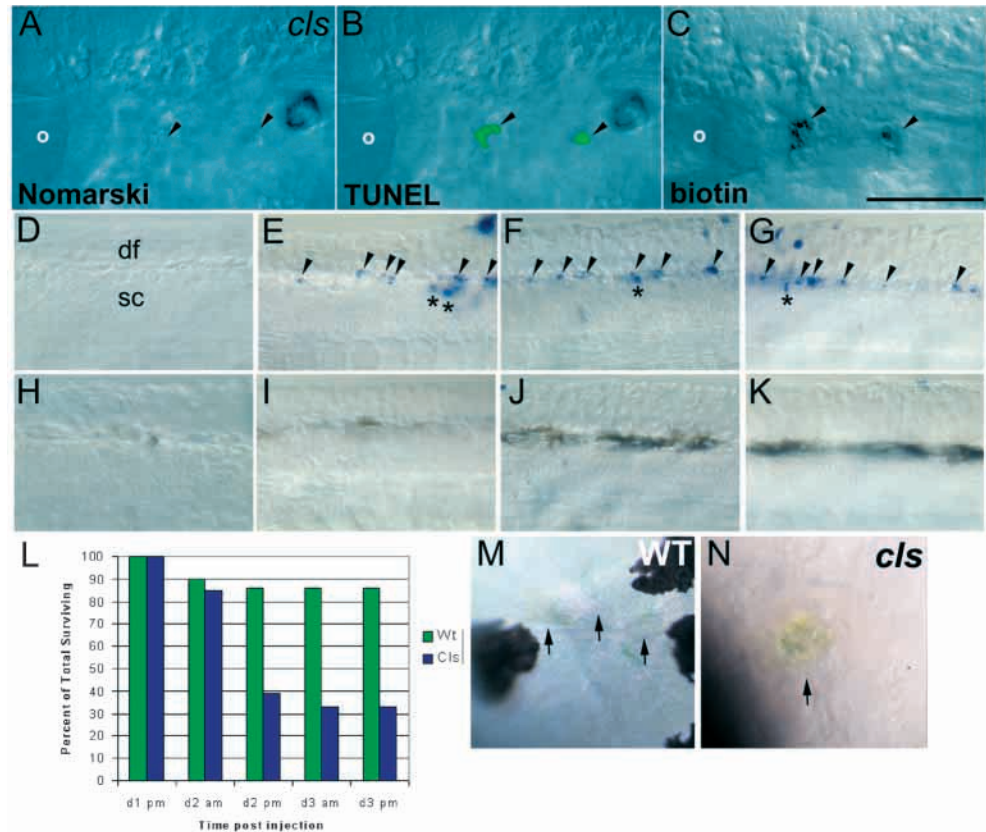
clones in *cls* embryos (45/49; 92%) died late on the second day (~35–45 hpf). Most showed no sign of morphological differentiation or pigmentation (34/49; 69%). The only exception, clones that developed some xanthophore pigmentation (11/49; 22%), always had abnormal morphology, being rather rounded and blebbed, and died soon after differentiation (Fig. 4N). A series of single cell injections in NCCs at the axial level of somite 7 gave similar results, with 92% of *cls* cells dying by around 48 hpf, in contrast to only 2% in wild-type siblings (data not shown); note that at this axial position no ectomesenchymal fates have been reported (Raible and Eisen, 1994). Our results are consistent with the severe reduction in differentiated non-ectomesenchymal fates in *cls* embryos and suggest that extensive NCC death is associated with the *cls* phenotype.

Non-ectomesenchymal crest derivatives die by apoptosis during a discrete time-window

The morphological appearance of dying cells in our clonal analyses suggested an apoptotic mechanism of death. We combined TUNEL with biotin-detection of the labelled clone in each of five *cls* embryos and showed that the dying cells had fragmented DNA (Fig. 4A–C). We conclude that many non-ectomesenchymal clones in *cls* embryos die by an apoptotic mechanism.

Analysis of cell survival in our cranial NCC data set shows that death of labelled NCCs occurs within a relatively discrete time-window (Fig. 4L). In both *cls* and wild-type embryos, around 10% of labelled clones had died by the morning after injection. In wild-type embryos, the number of surviving

Fig. 4. NCC death in *cls* embryos. (A-C) NCC clones die by an apoptotic mechanism in *cls* embryos. Lateral views of 40 hpf *cls* embryo in which two daughters of a single labelled NCC contributed to the posterior lateral line ganglion, lying just posterior to the otic vesicle (o). In the live embryo, both cells show blebbed morphology typical of apoptotic cells when viewed with Nomarski optics (A). After fixation and processing for TUNEL (B) and detection of the biotinylated-dextran lineage-tracer (C), visible TUNEL signal of these clonal cells indicates DNA fragmentation characteristic of apoptotic cells. (D-K) Whole-mount TUNEL shows NCC apoptosis in *cls* embryos. Lateral views of dorsal spinal cord (sc) in tail of 30 (D,H), 35 (E,I), 40 (F,J) and 45 (G,K) hpf embryos show apoptotic NCCs immediately dorsal to the spinal cord from 35 hpf in *cls* (arrowheads, D-G), but not wild-type (H-K), embryos. Scattered TUNEL-positive cells are prominent in dorsal spinal cord (*) of *cls* embryos (E-G); these are occasionally seen in wild-type siblings at these stages (data not shown). df, dorsal fin. (L) Time-course of labelled single cranial NCC clone survival in *cls* mutants and their wild-type siblings. Percentage of surviving clones is given at each of the five standard time points when embryos were examined. The time points correspond to approximately 16, 32, 40, 56 and 64 hpf, respectively. The first time point includes only single labelled NCCs based on examination within a few hours after labelling. See text for further details. (M,N) Wild-type xanthophores (arrows) at 48 hpf have a very flattened, thin morphology and are only weakly coloured (M), while a dying *cls* xanthophore (arrow) shows characteristic apoptotic morphology and concentrated yellow coloration, which was usually visible by 35 hpf (N). Scale bar: 100 μ m in A-C; 50 μ m in D-K; 75 μ m in M,N.



clones was essentially unchanged at later times. However, in *cls* mutants, the number of surviving clones dropped precipitously to only 40% within the period of around 5-10 hours between the two observational time-points on the second day after labelling (equivalent to ~40 hpf), but then remained constant. We interpret the early (overnight after injection) loss of wild-type and *cls* clones as representing death due to damage during labelling. The subsequent late loss of clones in *cls* embryos corresponds to the time of appearance of apoptotic cells and we attribute this to the *cls* phenotype.

To examine the extent to which apoptosis contributes to the *cls* phenotype, we used whole-mount TUNEL to examine apoptosis of NCCs (Fig. 4D-K). We saw a notable concentration of apoptotic cells dorsal or dorsolateral to the neural tube in *cls* embryos, but not in wild-type control embryos. A timecourse of TUNEL between 20 and 60 hpf indicated that cell death in NCCs becomes apparent by 35 hpf and continues to approximately 45 hpf.

***cls* neural crest cells fail to migrate before undergoing apoptosis**

Our *in vivo* clonal studies revealed that, while wild-type NCCs migrated extensively on both medial and lateral pathways, most *cls* NCCs failed to leave the premigratory crest area. Thus, excluding ectomesenchymal derivatives (which always

migrated normally), only 2/31 (6%) of cranial NCCs appeared to migrate away from their initial positions. At the level of somite 14, all wild-type labelled cells left the premigratory area, and more than 75% migrated at least 50 μ m from their original position. Only fin mesenchyme clones migrated normally in *cls* mutants. Of the remaining clones, only 4/23 (17%) migrated away from the premigratory crest; another cell extended towards the horizontal myoseptum, but maintained contact with the premigratory area. Of these five cells, two migrated on the lateral pathway, but underwent apoptosis after moving about half way to the horizontal myoseptum. The other three cells migrated on the medial path. In one case, the cell did not divide, migrated to a position appropriate for a dorsal root ganglion, then died before overt differentiation. The other two cells divided once; in each clone, one sister cell remained dorsal to the neural tube, and may have been an extramedullary cell (Kelsh and Eisen, 2000), while the other migrated to a dorsal root ganglial position, but failed to undergo axonogenesis, consistent with the impaired touch response of 5 dpf larvae. We obtained similar results for labelled NCCs from the region of somite 7 (data not shown). This direct observation of failed NCC migration in *cls* embryos is consistent with our observation of *dct*-expressing melanoblasts and *sox10*-expressing NCCs concentrated dorsal to the neural tube in mutant embryos (Kelsh et al., 2000b) (this work).

cls mutants and *sox10* morphants fail to express genes critical for melanophore specification and migration

cls mutants combine an extensive failure of NCC migration with late apoptotic death of non-ectomesenchymal derivatives. Three recent studies suggested a possible molecular genetic mechanism for these aspects of the phenotype. *sparse* (*spa*), a *kit* homologue, is crucial for survival and migration of melanophores and melanoblasts (Parichy et al., 1999; Kelsh et al., 2000b) and *nacre* (*nac*), a *microphthalmia transcription factor* (*mitf*) homologue, is crucial for melanophore specification and required for *spa* expression (Lister et al., 1999). We used in situ hybridisation at 20–35 hpf to ask whether *spa* or *nac* expression was disrupted in *cls* embryos (Fig. 5). We found that both *spa* and *nac* expression were absent from NCCs, even at a time when many *dct*-positive cells are present, suggesting that the *cls* melanophore phenotype might result from loss of *nac* expression. By contrast, *spa* expression in intermediate cell mass and *nac* expression in the pigmented retinal epithelium are unaffected in *cls* mutants.

We have recently shown that injection of *sox10* morpholino oligonucleotides phenocopies the *cls* mutant phenotype (Dutton et al., 2001). The morphant phenotype varies depending upon the amount of morpholino injected, with high doses phenocopying all aspects of the phenotype of the strong *cls* alleles. Injection of lower doses results in a phenocopy of the weak *cls* allele phenotype, with embryos showing some melanophores, concentrated in dorsal positions (Dutton et al., 2001; Malicki et al., 1996). The number of *nac/mitf*-expressing cells in embryos injected with a low dose of *sox10* morpholino (median number=78; $n=20$) is significantly higher than in embryos injected with a high dose (median number=20; $n=20$; Mann-Whitney U-test, $P<0.05$; Fig. 5C,D), consistent with the differences in melanophore phenotype.

DISCUSSION

Studies in mice have led to identification of *Sox10* as a key gene in human Waardenburg-Shah syndrome. We have shown that the zebrafish *cls* locus is a *sox10* homologue predicted to encode a protein with all the major domains identified in mammals (Fig. 1). We have identified the molecular lesion likely to cause the mutant phenotype in 4 *cls* alleles. In two cases, *tw2* and *tw11*, both originating from the same mutagenised male (Haffter et al., 1996; Kelsh et al., 1996), the lesions are identical and are presumably independent isolations of the same allele. The zebrafish Lys376Stop lesions resemble the human 059 allele (delGA) in lacking the transactivation domain, although they lack the C-terminal extension present in the human allele. In transient transfection assays human 059 mutant protein has been shown to have no transcriptional activation (Bondurand et al., 2000; Kuhlbrodt et al., 1998b; Liu et al., 1999). The *m618* allele substitutes Leu142 in the second alpha helix of the HMG domain and there is no similar mammalian mutation. The *t3* allele results in a severely truncated protein that lacks both the DNA-binding and transcriptional activation domains. It is thus reminiscent of the human Y83X allele which has been proposed to be a functional null (Kuhlbrodt et al., 1998b; Potterf et al., 2000). All four mutant alleles described here show similar, strong phenotypes

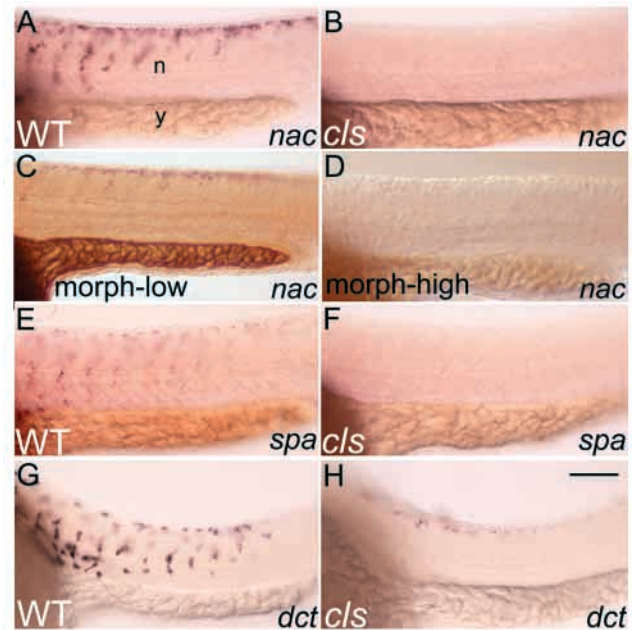


Fig. 5. *cls* mutants lack *nac* and *spa* expression. Lateral views of caudal trunk of 25 hpf wild-type and *cls* embryos after in situ hybridisation with *nac* (A,B), *spa* (E,F) and *dct* (G,H) probes. (C,D) *nac/mitf* expression is decreased weakly (C) or strongly (D) after injection with either a low or high dose, respectively, of *sox10* morpholino. n, neural tube; y, yolk sac. Scale bar: 75 μ m.

(Kelsh et al., 1996; Malicki et al., 1996) (data not shown). These considerations, combined with the similarity of these phenotypes with the maximal morphant phenocopy generated with a *sox10* morpholino, lead us to suggest that these alleles are all likely null alleles. Analysis of the activities of these mutant proteins will be interesting to test this proposal.

Zebrafish *sox10* expression is consistent with cell types affected in *cls* mutants and strongly reminiscent of that in mammals. We have taken advantage of the higher resolution of such studies in zebrafish, to define more precisely the extent of *sox10* expression throughout the neural crest at different stages. In wild type, expression is extensive in premigratory neural crest, but comparison with *fdk6* expression shows that a minority of premigratory NCCs lack *sox10* expression. Expression persists in some migrating cells on the medial migration pathway, but is rapidly downregulated in differentiating pigment cells. Glia of the developing peripheral nervous system show strong expression, as has also been described in mice (Kuhlbrodt et al., 1998a; Britsch et al., 2001). Crest cells in forming branchial arches and fin mesenchyme do not show expression, in agreement with mouse, but not human, expression studies (Bondurand et al., 1998; Kuhlbrodt et al., 1998a; Southard-Smith et al., 1998). Late expression in cranial cartilages is intriguing, but will require further study to evaluate its role. In *cls* mutants, *sox10*-expression in premigratory NCCs is initially unaffected but, unlike in wild-type siblings, *sox10*-expressing cells soon accumulate in this position. In the trunk *sox10*-expressing cells migrating on the medial pathway are seen and presumably contribute to the neurones and glia of the dorsal root ganglia, which are detectable in mutants (Kelsh and Eisen, 2000) (this

study). NCCs tend to become clustered in premigratory positions in *cls* mutants, consistent with the observed defect in NCC migration revealed by our single-cell labelling studies.

Outside the neural crest, *sox10* expression is also largely conserved. Thus, expression in the developing inner ear epithelium is seen in zebrafish as well as in mammals (Bondurand et al., 1998; Southard-Smith et al., 1998). In zebrafish, this expression is remarkably strong and persistent in wild type, but is downregulated in *cls* mutants by 40 hpf. As pronounced otic defects are morphologically detectable in *cls* mutants by 48 hpf (R. N. K., unpublished), we suggest that *sox10* is crucial for development of otic epithelium. Limited expression in embryonic central nervous system is seen in zebrafish and mice (Kuhlbrodt et al., 1998a), although detailed studies will be required to establish the cell types involved in each case.

Our single cell labelling studies at three rostrocaudal positions make clear that defects in *cls* mutants are not limited to one axial position, but instead affect non-ectomesenchymal rather than ectomesenchymal crest derivatives. Most NCCs in *cls* mutants show restricted migration and poor or no differentiation before dying by an apoptotic mechanism within a discrete time-window. We interpret the dying cells as being those that would in wild-type siblings form non-ectomesenchymal fates. Thus, in *cls* embryos, NCCs that would normally yield these missing neural crest derivatives are present in premigratory neural crest in normal numbers, but then die before differentiating, usually without migrating. This confirms and extends reports that putative NCCs apoptose during migration in mouse *sox10* mutants (Kapur, 1999; Southard-Smith et al., 1998).

The *sox10* expression pattern in *cls* mutants may appear contradictory to our single cell label results, as the expression studies show normal numbers of *sox10*-positive NCCs migrating on the medial pathway, while the single cell labelling studies show a strong migration defect in the neural crest. However, our data suggest that *sox10* is expressed in almost all premigratory cells, but is rapidly downregulated in ectomesenchymal and pigment cell precursors as they start to migrate. Thus, *sox10* expression in migrating cells reflects just the neural precursors. Our studies show that these cells are much less defective in migration in *cls* mutants. Consistent with this, the labelled cells in *cls* mutants that did migrate normally all took the medial migration pathway and, if they survived, adopted a position consistent with a dorsal root ganglial fate. By contrast, most labelled NCC clones generated pigment cells, consistent with former studies in zebrafish. These pigment cells are severely defective in migration, as shown by molecular markers for xanthophore (*gdh*; Parichy et al., 2000) and melanophore (*dcr*; Fig. 5) cell fates (M. Hawkins and R. N. K., unpublished) (Kelsh and Eisen, 2000). Further work will be required to investigate the specification status of the migrating neural precursors in wild-type and mutant embryos.

We have demonstrated the complexity of NCC defects in *cls* embryos, with survival, migration and differentiation of non-ectomesenchymal cell types all affected. Further, a small decrease in clone size suggests that proliferation may also be somewhat affected (K. A. D. and R. N. K., unpublished). This spectrum of defects is not readily consistent with a primary function for wild-type *cls/sox10* in NCC survival, proliferation

or differentiation. Although a dying cell might show abnormal migration and proliferation, the timing of appearance of defects in *cls* mutants conflicts with cell survival being the primary defect. We can first distinguish *cls* mutants at 20 hpf (by lack of *nac/mitf* expression), but do not see NCC apoptosis by TUNEL until around 35 hpf; previous work in zebrafish has suggested that the delay between induction of apoptosis and detectable morphological changes and DNA fragmentation is at most 3-4 hours (Ikegami et al., 1999). Likewise the *cls* mutant phenotype cannot be explained as primarily a failure of migration, with subsequent failure of exposure to required trophic factors, because for three subsets of affected cells (three pigment cell types in the stripe dorsal to the neural tube), the premigratory position is also a final location and hence the necessary trophic factors must be available. Despite this, in *cls* mutants all pigment cells, including those of the dorsal stripe, fail to develop properly. Instead, we propose that the primary role of *cls* gene function is in specification of non-ectomesenchymal cell fates; all other defects in *cls* mutants would then be secondary effects of a failure to become properly specified. Thus, in *cls* mutants NCCs are unable to adopt non-ectomesenchymal fates and so fail to differentiate. This differentiation process would include expression of growth and trophic factor receptors, and hence secondary defects might include impaired proliferation and later apoptosis. Our identification of the *cls* gene as a *sox10* transcription factor gene is consistent with this interpretation.

Indeed, for the specific case of melanophore fate, data presented here and elsewhere permit us to propose a molecular model consistent with this interpretation (Fig. 6). In both zebrafish and mammals, *Nac/Mitf* homologues have been shown to be important transcription factors for specifying melanophore fate (Lister et al., 1999; Opdecamp et al., 1997; Tachibana et al., 1996). We show here that *cls* mutants lack expression of *nac* (indeed it is the earliest defect we have identified). Thus, *sox10* is required for *nac* expression and thus for melanophore lineage specification. In addition, in *nac* mutants, *nac*-positive cells show a failure to migrate highly reminiscent of the *cls* melanoblast phenotype (Lister et al., 1999). Likewise, in both *cls* and *nac* mutants, *spa/kit* expression is lost in melanoblasts. *spa* function is necessary for both melanoblast migration and melanoblast and melanophore survival (Kelsh et al., 2000b; Parichy et al., 1999). Furthermore, the timing of loss of melanoblasts in *spa* mutants, beginning between 30 and 36 hpf, is consistent with the timing of decrease in melanoblast numbers and with the timing of NCC apoptosis in *cls* mutants (Kelsh et al., 2000b; this study). Hence, a simple model can largely explain the *cls* melanophore phenotype. *cls/sox10* has a key role, by direct or indirect activation of *nac/mitf*, in melanophore specification and consequently *cls* mutants lack expression of genes activated by *nac*, including *spa/kit*, mediating survival and migration, and melanogenic enzymes, mediating pigmentation. In support of this model, injection of *sox10* mRNA into early embryos results in ectopic *nac/mitf* expression and expression of *nac* in *cls* embryos is sufficient to rescue melanophores (S. E. and R. N. K., unpublished). It will be of interest to expand this model to include other targets of *sox10* and *nac*, as well as to extend this model to other non-ectomesenchymal neural crest derivatives affected in *cls* mutants. Our model predicts that the immediate targets of *sox10* will be either master regulators of

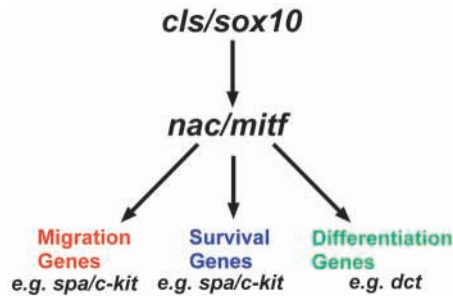


Fig. 6. Model of role of *cls/sox10* in melanophore specification. Formal genetic interactions between selected genes known to function in zebrafish melanophore development are schematised. In *cls* mutants, failure to activate *nac* expression (and thus to specify melanophore fate) results in absence of gene products critical for melanophore survival, migration and differentiation. For details, see main text.

neural crest fate (e.g. *nac*) or a multitude of diverse gene products required within specific crest derivatives for the cellular functions of trophic support, migration and differentiation. Thus, it will be important to identify the direct targets of Sox10 transcriptional regulation.

This specific model is likely to be applicable to mammalian neural crest too. Thus, Sox10 directly regulates *Mitf* expression in mouse (Bondurand et al., 2000; Lee et al., 2000; Potterf et al., 2000; Verastegui et al., 2000). Although *Dct*-positive melanoblasts are not detectable in *Sox10^{Dom}* mice, some evidence of impaired or delayed migration of some NCCs has been presented (Southard-Smith et al., 1998). Similarly, *Kit* function is critically involved in promoting melanoblast migration and survival, is rapidly lost from melanoblasts in *Mitf* mutants and is known to be a direct target of Mitf, at least in cultured mast cells (Opdecamp et al., 1997; Wehrle-Haller and Weston, 1995; Wehrle-Haller and Weston, 1997). In *Sox10* mutant mice, *Kit* expression in melanoblasts may be absent, although the presence of unaffected cells in the skin, suggested to be mast cells, means that this result needs to be confirmed (Bondurand et al., 2000).

sox10 alone cannot be sufficient to specify each of the non-ectomesenchymal fates. We believe that *sox10*, while crucial for each of them, is not sufficient; instead, we propose that *sox10* is one of a combination of genes that together specify non-ectomesenchymal fates from neural crest. This model helps explain why cells that express molecular markers for affected cell types can be identified in *cls* mutants (Kelsh and Eisen, 2000). For example, although melanophores barely express melanin, xanthophores show much pigment in *cls* mutants. If a combination of transcription factors together specify a cell type, each factor might regulate only partially overlapping subsets of the characteristics of individual fates. In the absence of *sox10* gene function, those aspects of melanophore and xanthophore fate requiring *sox10* function would be affected (e.g. synthesis of melanin and trophic machinery, respectively), while others would remain at least partly unaffected (e.g. *dct* expression and pteridine pigment synthesis, respectively). A directly analogous mechanism has been proposed for autonomic neurone specification from the neural crest, with different genes regulating pan-neuronal and subtype specific cell properties (Anderson et al., 1997). Factors that interact with Sox10 to regulate target genes have been

described, including the paired box transcription factor Pax3 and the POU-domain protein Tst-1/Oct6/SCIP (Bondurand et al., 2000; Kuhlbrodt et al., 1998a). However, it remains to be seen whether these co-factors have any role in distinguishing non-ectomesenchymal fates. Identification of combinations of transcription factors required to specify each fate will be a promising line of future research.

Our specification model predicts that *sox10* function is required only in NCCs fated to non-ectomesenchymal derivatives. *fkf6* is expressed very broadly in premigratory NCCs (Odenthal and Nuesslein-Volhard, 1998) and shows extensive, but incomplete, overlap with *sox10*. Further studies will be required to test whether *sox10*-; *fkf6*+ NCCs represent ectomesenchymal precursors. However, our results do show that, consistent with our model, expression is, at least, rapidly downregulated in cells that adopt ectomesenchymal fates. In mammals, *Sox10* has sometimes been assumed to be a generic NCC marker (Pattyn et al., 1999), but our results show that, in fish, overlap with other NC markers is incomplete, even at premigratory stages.

In many respects, zebrafish neural crest development is typical of neural crest development in all vertebrates (Raible et al., 1992). In contrast to mouse and human *Sox10* mutations, none of the fish *sox10* mutations show dominant effects on melanophore number or pattern (R. N. K., unpublished). In mice, expressivity of the *sox10* haploinsufficiency phenotype is dependent on the genetic background (Lane and Liu, 1984). Presumably, in the AB background in zebrafish heterozygotes have sufficient Sox10 for normal melanophore development. Nevertheless, the conserved expression pattern and homozygous phenotypes in the two species suggest that the detailed cell-biological basis for the *cls* phenotype proposed here illuminates a possible mechanism behind Waardenburg-Shah syndrome and Hirschsprung's disease, in which reduced SOX10 function may reduce the number of melanoblasts and enteric precursors specified.

We thank J. James for fish husbandry, L. D. Hurst for generation of Fig. 1B, D. Raible for pCSHSP, and C. Miller, D. Parichy and D. Raible for cDNA clones. We also gratefully acknowledge J. Eisen, D. Raible, J. M. W. Slack, R. Adams, W. Bennett, A. Ward and J. R. Dutton for helpful criticism and discussion of the manuscript. R. G. thanks S. Rudolph-Geiger for technical assistance. This work was supported by a Praxis XXI PhD Studentship (S. S. L.), a University of Bath studentship and ORS award (T. J. C.), a Royal Society Research Grant, Wellcome Trust Project Grant 050602/Z, a MRC Co-operative Group Component Grant G9810985, and MRC Co-operative Group Grant G9721903. R. G. and P. H. were supported by the German Human Genome Project (DHGP Grant 01 KW 9919).

REFERENCES

- Akimenko, M. A., Ekker, M., Wegner, J., Lin, W. and Westerfield, M. (1994). Combinatorial expression of three zebrafish genes related to distal-less: part of a homeobox gene code for the head. *J. Neurosci.* **14**, 3475-3486.
- Anderson, D. J., Groves, A., Lo, L., Rao, M., Shah, N. M. and Sommer, L. (1997). Cell lineage determination and the control of neuronal identity in the crest. *Cold Spring Harbor Symp. Quant. Biol.* **LXII**, 493-504.
- Attíe, T., Till, M., Pelet, A., Amiel, J., Edery, P., Boutrand, L., Munnich, A. and Lyonnet, S. (1995). Mutation of the endothelin-receptor B gene in Waardenburg-Hirschsprung disease. *Hum. Mol. Genet.* **4**, 2407-2409.
- Baynash, A. G., Hosoda, K., Giaid, A., Richardson, J. A., Emoto, N.,

- Hammer, R. E. and Yanagisawa, M. (1994). Interaction of endothelin-3 with endothelin-B receptor is essential for development of epidermal melanocytes and enteric neurons. *Cell* **79**, 1277-1285.
- Bolande, R. P. (1974). The neurocristopathies: a unifying concept of disease arising in neural crest maldevelopment. *Hum. Pathol.* **5**, 409-429.
- Bondurand, N., Kobetz, A., Pingault, V., Lemort, N., EnchaRazavi, F., Couly, G., Goerich, D. E., Wegner, M., Abitbol, M. and Goossens, M. (1998). Expression of the SOX10 gene during human development. *FEBS Lett.* **432**, 168-172.
- Bondurand, N., Pingault, V., Goerich, D. E., Lemort, N., Sock, E., Caigec, C. L., Wegner, M. and Goossens, M. (2000). Interaction among SOX10, PAX3 and MITF, three genes altered in Waardenburg syndrome. *Hum. Mol. Genet.* **9**, 1907-1917.
- Britsch, S., Goerich, D. E., Riethmacher, D., Peirano, R. I., Rossner, M., Nave, K. A., Birchmeier, C. and Wegner, M. (2001). The transcription factor Sox10 is a key regulator of peripheral glial development. *Genes Dev.* **15**, 66-78.
- Dutton, K., Dutton, J. R., Pauliny, A. and Kelsh, R. N. (2001). A morpholino phenocopy of the *colourless* mutant. *Genesis* **30**, 188-189.
- Ederly, P., Atti'e, T., Amiel, J., Pelet, A., Eng, C., Hofstra, R. M., Martelli, H., Bidaud, C., Munnich, A. and Lyonnet, S. (1996). Mutation of the endothelin-3 gene in the Waardenburg-Hirschsprung disease (Shah-Waardenburg syndrome). *Nat. Genet.* **12**, 442-444.
- Haffter, P., Granato, M., Brand, M., Mullins, M., Hammerschmidt, M., Kane, D., Odenthal, J., van Eeden, F., Jiang, Y., Heisenberg, C. et al. (1996). The identification of genes with unique and essential functions in the development of the zebrafish, *Danio rerio*. *Development* **123**, 1-36.
- Halloran, M., Sato-Maeda, M., Warren, J., Su, F., Lele, Z., Krone, P., Kuwada, J. and Shoji, W. (2000). Laser-induced gene expression in specific cells of transgenic zebrafish. *Development* **127**, 1953-1960.
- Herbarth, B., Pingault, V., Bondurand, N., Kuhlbrodt, K., Hermans-Borgmeyer, I., Puliti, A., Lemort, N., Goossens, M. and Wegner, M. (1998). Mutation of the Sry-related Sox10 gene in Dominant megacolon, a mouse model for human Hirschsprung disease. *Proc. Natl. Acad. Sci. USA* **95**, 5161-5165.
- Hofstra, R. M., Osinga, J., Tan Sindhunata, G., Wu, Y., Kamsteeg, E. J., Stulp, R. P., van Ravenswaaij Arts, C., Majoor Krakauer, D., Angrist, M., Chakravarti, A. et al. (1996). A homozygous mutation in the endothelin-3 gene associated with a combined Waardenburg type 2 and Hirschsprung phenotype (Shah-Waardenburg syndrome). *Nat. Genet.* **12**, 445-447.
- Hosoda, K., Hammer, R. E., Richardson, J. A., Baynash, A. G., Cheung, J. C., Giaid, A. and Yanagisawa, M. (1994). Targeted and natural (piebald-lethal) mutations of endothelin-B receptor gene produce megacolon associated with spotted coat color in mice. *Cell* **79**, 1267-1276.
- Hukriede, N. A., Joly, L., Tsang, M., Miles, J., Tellis, P., Epstein, J. A., Barbazuk, W. B., Li, F. N., Paw, B., Postlethwait, J. H. et al. (1999). Radiation hybrid mapping of the zebrafish genome. *Proc. Natl. Acad. Sci. USA* **96**, 9745-9750.
- Ikegami, R., Hunter, P. and Yager, T. D. (1999). Developmental activation of the capability to undergo checkpoint-induced apoptosis in the early zebrafish embryo. *Dev. Biol.* **209**, 409-433.
- Kapur, R. P. (1999). Early death of neural crest cells is responsible for total enteric aganglionosis in Sox10(Dom)/Sox10(Dom) mouse embryos. *Pediatr. Dev. Pathol.* **2**, 559-569.
- Kelsh, R. N., Brand, M., Jiang, Y.-J., Heisenberg, C. P., Lin, S., Haffter, P., Odenthal, J., Mullins, M. C., van Eeden, F. J., Furutani-Seiki, M. et al. (1996). Zebrafish pigmentation mutations and the processes of neural crest development. *Development* **123**, 369-389.
- Kelsh, R. N. and Eisen, J. S. (2000). The zebrafish *colourless* gene regulates development of non-ectomesenchymal neural crest derivatives. *Development* **127**, 515-525.
- Kelsh, R. N., Dutton, K., Medlin, J. and Eisen, J. S. (2000a). Expression of zebrafish *fd6* in neural crest-derived glia. *Mech. Dev.* **93**, 161-164.
- Kelsh, R. N., Schmid, B. and Eisen, J. S. (2000b). Genetic analysis of melanophore development in zebrafish embryos. *Dev. Biol.* **225**, 277-293.
- Kimmel, C. B., Ballard, W. W., Kimmel, S. R., Ullmann, B. and Schilling, T. F. (1995). Stages of embryonic development of the zebrafish. *Dev. Dyn.* **203**, 253-310.
- Knapik, E., Goodman, A., Atkinson, O., Roberts, C., Shiozawa, M., Sim, C., Weksler-Zangen, S., Trolliet, M., Futrell, C., Innes, B. et al. (1996). A reference cross DNA panel for zebrafish (*Danio rerio*) anchored with simple sequence length polymorphisms. *Development* **123**, 451-460.
- Kuhlbrodt, K., Herbarth, B., Sock, E., Hermans-Borgmeyer, I. and Wegner, M. (1998a). Sox10, a novel transcriptional modulator in glial cells. *J. Neurosci.* **18**, 237-250.
- Kuhlbrodt, K., Schmidt, C., Sock, E., Pingault, V., Bondurand, N., Goossens, M. and Wegner, M. (1998b). Functional analysis of Sox10 mutations found in human Waardenburg-Hirschsprung patients. *J. Biol. Chem.* **273**, 23033-23038.
- Lane, P. W. and Liu, H. M. (1984). Association of megacolon with a new dominant spotting gene (Dom) in the mouse. *J. Hered.* **75**, 435-439.
- Le Douarin, N. M. (1982). *The Neural Crest*. Cambridge: Cambridge University Press.
- Lee, M., Goodall, J., Verastegui, C., Ballotti, R. and Goding, C. R. (2000). Direct regulation of the microphthalmia promoter by Sox10 links Waardenburg-Shah syndrome (WS4)-associated hypopigmentation and deafness to WS2. *J. Biol. Chem.* **275**, 37978-37983.
- Lister, J. A., Robertson, C. P., Lepage, T., Johnson, S. L. and Raible, D. W. (1999). nacre encodes a zebrafish microphthalmia-related protein that regulates neural-crest-derived pigment cell fate. *Development* **126**, 3757-3767.
- Liu, Q., Melnikova, I. N., Hu, M. and Gardner, P. D. (1999). Cell type-specific activation of neuronal nicotinic acetylcholine receptor subunit genes by Sox10. *J. Neurosci.* **19**, 9747-9755.
- Malicki, J., Schier, A. F., Solnica-Krezel, L., Stemple, D. L., Neuhauss, S. C. F., Stainier, D. Y. R., Abdelilah, S., Rangini, Z., Zwartkruis, F. and Driever, W. (1996). Mutations affecting development of the zebrafish ear. *Development* **123**, 275-283.
- Marusich, M. F., Furneaux, H. M., Henion, P. D. and Weston, J. A. (1994). Hu neuronal proteins are expressed in proliferating neurogenic cells. *J. Neurobiol.* **25**, 143-155.
- Mayer, T. C. (1965). The development of piebald spotting in mice. *Dev. Biol.* **11**, 319-334.
- Mayer, T. C. and Maltby, E. L. (1964). An experimental investigation of pattern development in lethal spotting and belted mouse embryos. *Dev. Biol.* **9**, 269-286.
- Odenthal, J. and Nusslein-Volhard, C. (1998). *fork head* domain genes in zebrafish. *Dev. Genes Evol.* **208**, 245-258.
- Opdecamp, K., Nakayama, A., Nguyen, M. T. T., Hodgkinson, C. A., Pavan, W. J. and Arnheiter, H. (1997). Melanocyte development in vivo and in neural crest cell cultures: Crucial dependence on the Mitf basic-helix-loop-helix-zipper transcription. *Development* **124**, 2377-2386.
- Parichy, D. M., Rawls, J. F., Pratt, S. J., Whitfield, T. T. and Johnson, S. L. (1999). Zebrafish sparse corresponds to an orthologue of c-kit and is required for the morphogenesis of a subpopulation of melanocytes, but is not essential for hematopoiesis or primordial germ cell development. *Development* **126**, 3425-3436.
- Parichy, D. M., Ransom, D. G., Paw, B., Zon, L. I. and Johnson, S. L. (2000). An orthologue of the kit-related gene *fms* is required for development of neural crest-derived xanthophores and a subpopulation of adult melanocytes in the zebrafish, *Danio rerio*. *Development* **127**, 3031-3044.
- Pattyn, A., Morin, X., Cremer, H., Goridis, C. and Brunet, J.-F. (1999). The homeobox gene *Phox2b* is essential for the development of autonomic neural crest derivatives. *Nature* **399**, 366-370.
- Peirano, R. I. and Wegner, M. (2000). The glial transcription factor Sox10 binds to DNA both as monomer and dimer with different functional consequences. *Nucleic Acids Res.* **28**, 3047-3055.
- Pevny, L. H. and Lovell-Badge, R. (1997). Sox genes find their feet. *Curr. Opin. Genet. Dev.* **7**, 338-44.
- Pingault, V., Bondurand, N., Kuhlbrodt, K., Goerich, D. E., Prehu, M. O., Puliti, A., Herbarth, B., Hermans-Borgmeyer, I., Legius, E., Matthijs, G. et al. (1998). SOX10 mutations in patients with Waardenburg-Hirschsprung disease. *Nat. Genet.* **18**, 171-173.
- Potterf, S. B., Furumura, M., Dunn, K. J., Arnheiter, H. and Pavan, W. J. (2000). Transcription factor hierarchy in Waardenburg syndrome: regulation of MITF expression by SOX10 and PAX3. *Hum. Genet.* **107**, 1-6.
- Puffenberger, E. G., Hosoda, K., Washington, S. S., Nakao, K., deWit, D., Yanagisawa, M. and Chakravarti, A. (1994). A missense mutation of the endothelin-B receptor gene in multigenic Hirschsprung's disease. *Cell* **79**, 1257-1266.
- Pusch, C., Huster, E., Pfeifer, D., Sudbeck, P., Kist, R., Roe, B., Wang, Z., Balling, R., Blin, N. and Scherer, G. (1998). The SOX10/Sox10 gene from human and mouse: sequence, expression, and transactivation by the encoded HMG domain transcription factor. *Hum. Genet.* **103**, 115-123.
- Raible, D. W. and Eisen, J. S. (1994). Restriction of neural crest cell fate in the trunk of the embryonic zebrafish. *Development* **120**, 495-503.

- Raible, D. W., Wood, A., Hodsdon, W., Henion, P. D., Weston, J. A. and Eisen, J. S. (1992). Segregation and early dispersal of neural crest cells in the embryonic zebrafish. *Dev. Dyn.* **195**, 29-42.
- Rauch, G. J., Hammerschmidt, M., Blader, P., Schauerte, H. E., Strahle, U., Ingham, P. W., McMahon, A. P. and Hafter, P. (1997). Wnt5 is required for tail formation in the zebrafish embryo. *Cold Spring Harbor Symp. Quant. Biol.* **62**, 227-234.
- Reyes, R. (1999). Development and Death of Zebrafish Rohon-Beard Spinal Sensory Neurons. In *Institute of Neuroscience*, pp. 1-99. Eugene, OR: University of Oregon.
- Schilling, T. F. and Kimmel, C. B. (1994). Segment and cell type lineage restrictions during pharyngeal arch development in the zebrafish embryo. *Development* **120**, 483-494.
- Schulte-Merker, S., Van Eeden, F. J. M., Halpern, M. E., Kimmel, C. B. and Nüsslein-Volhard, C. (1994). *no tail (ntl)* is the zebrafish homologue of the mouse *T (Brachyury)* gene. *Development* **120**, 1009-1015.
- Smith, M., Hickman, A., Amanze, D., Lumsden, A. and Thorogood, P. (1994). Trunk neural crest origin of caudal fin mesenchyme in the zebrafish *Brachydanio rerio*. *Proc. R. Soc. London B Biol. Sci.* **256**, 137-145.
- Southard-Smith, E. M., Kos, L. and Pavan, W. J. (1998). Sox10 mutation disrupts neural crest development in DOM Hirschsprung mouse model. *Nat. Genet.* **18**, 60-64.
- Southard-Smith, E. M., Angrist, M., Ellison, J. S., Agarwala, R., Baxevanis, A. D., Chakravarti, A. and Pavan, W. J. (1999). The Sox10(Dom) mouse: modeling the genetic variation of Waardenburg-Shah (WS4) syndrome. *Genome Res.* **9**, 215-225.
- Strimmer, K. and von Haeseler, A. (1996). Quartet puzzling: A quartet maximum-likelihood method for reconstructing tree topologies. *Mol. Biol. Evol.* **13**, 964-969.
- Tachibana, M., Takeda, K., Nobukuni, Y., Urabe, K., Long, J. E., Meyers, K. A., Aaronson, S. A. and Miki, T. (1996). Ectopic expression of MITF, a gene for Waardenburg syndrome type 2, converts fibroblasts to cells with melanocyte characteristics. *Nature Genet.* **14**, 50-54.
- Tamura, K. and Nei, M. (1993). Estimation of the number of nucleotide substitutions in the control region of mitochondrial-DNA in humans and chimpanzees. *Mol. Biol. Evol.* **10**, 512-526.
- Thompson, J. D., Gibson, T. J., Plewniak, F., Jeanmougin, F. and Higgins, D. G. (1997). The CLUSTAL_X windows interface: flexible strategies for multiple sequence alignment aided by quality analysis tools. *Nucleic Acids Res.* **25**, 4876-4882.
- Verastegui, C., Bille, K., Ortonne, J. P. and Ballotti, R. (2000). Regulation of microphthalmia-associated transcription factor gene by the waardenburg syndrome type 4 Gene, Sox10. *J. Biol. Chem.* **275**, 30757-60.
- Wegner, M. (1999). From head to toes: the multiple facets of Sox proteins. *Nucleic Acids Res.* **27**, 1409-1420.
- Wehrle-Haller, B. and Weston, J. A. (1995). Soluble and cell-bound forms of steel factor activity play distinct roles in melanocyte precursor dispersal and survival on the lateral neural crest migration pathway. *Development* **121**, 731-742.
- Wehrle-Haller, B. and Weston, J. A. (1997). Receptor tyrosine kinase-dependent neural crest migration in response to differentially localized growth factors. *BioEssays* **19**, 337-345.
- Yuan, H., Corbi, N., Basilico, C. and Dailey, L. (1995). Developmental-specific activity of the FGF-4 enhancer requires the synergistic action of Sox2 and Oct-3. *Genes Dev.* **9**, 2635-2645.